THE JOURNAL OF PHYSICAL CHEMISTRY LETTERS
A JOURNAL OF THE AMERICAN CHEMICAL SOCIETY

pubs.acs.org/JPCL

Letter

Cancer-Related Mutations Alter RNA-Driven Functional Cross-Talk Underlying Premature-Messenger RNA Recognition by Splicing Factor SF3b

Angelo Spinello, Pavel Janos, Riccardo Rozza, and Alessandra Magistrato*

Cite This: *J. Phys. Chem. Lett.* 2023, 14, 6263−6269

Read Online

ACCESS | Metrics & More | Article Recommendations | Supporting Information

ABSTRACT: The pillar of faithful premature-messenger (pre-mRNA) splicing is the precise recognition of key intronic sequences by specific splicing factors. The heptameric splicing factor 3b (SF3b) recognizes the branch point sequence (BPS), a key part of the 3′ splice site. SF3b contains SF3B1, a protein holding recurrent cancer-associated mutations. Among these, K700E, the most-frequent SF3B1 mutation, triggers aberrant splicing, being primarily implicated in hematologic malignancies. Yet, K700E and the BPS recognition site are 60 Å apart, suggesting the existence of an allosteric cross-talk between the two distal spots. Here, we couple molecular dynamics simulations and dynamical network theory analysis to unlock the molecular terms underpinning the impact of SF3b splicing factor mutations on pre-mRNA selection. We establish that by weakening and remodeling interactions of pre-mRNA with SF3b, K700E scrambles RNA-mediated allosteric cross-talk between the BPS and the mutation site. We propose that the altered allostery contributes to cancer-associated missplicing by mutated SF3B1. This finding broadens our comprehension of the elaborate mechanisms underlying pre-mRNA metabolism in eukaryotes.

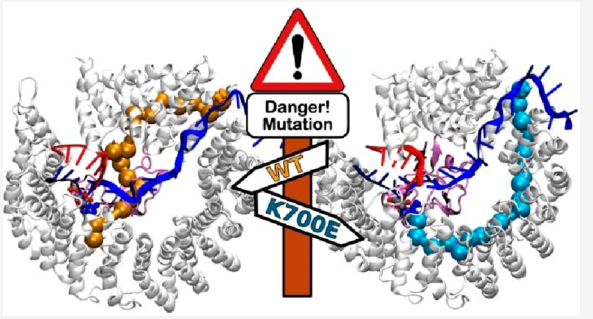

Pre-mRNA splicing, a pivotal step of gene expression and diversification, is catalyzed by the spliceosome, an extraordinarily complex macromolecular machinery composed of hundreds of proteins and five small nuclear RNAs (snRNAs).[1] The spliceosome converts a premature-messenger (pre-m)RNA strand into its mature functional form (mRNA) and long noncoding RNAs by removing intervening intronic sequences and joining the remaining exons.[2,3] To ensure splicing fidelity and maintain proteome integrity, critical pre-mRNA sequences must be precisely recognized.[4] These are the 5′ and 3′ splice sites, the branch point sequence,[5] and the polypyrimidine tract, located at the exons/introns boundaries and within the introns, respectively.[6] However, the situation is even more complex since pre-mRNAs can undergo alternative splicing patterns, whereby some exons can be skipped or some introns can be retained.

Dysregulation of pre-mRNA recognition is associated with several diseases (i.e., cancer, neurodegeneration, and genetic disorders).[7] Indeed, recurrent splicing factor mutations alter the selection of pre-mRNA signaling sequences.[8] Mutations of splicing factors are recurrently found in patient-derived samples of hematological malignancies (e.g., myelodysplastic syndrome, chronic lymphocytic leukemia, and chronic myelomonocytic leukemia)[9] while being less common in solid tumors (e.g., breast cancer and uveal melanoma).[10]

The heptameric splicing factor 3b (SF3b), a component of the U2 small nuclear ribonucleoproteins (snRNP), recognizes a degenerate branch point sequence, containing a conserved branch point adenosine (BPA) that serves as a nucleophile in the first splicing step.[2,3] The BPA binds at the interface of the SF3b proteins SF3B1 and PHF5A. SF3B1 contains an intrinsically disordered N-terminal region (residues 1−400) and a solenoidal C-terminal region with 20 leucine-rich HEAT domains (the acronym comes from Huntingtin, elongation factor 3, the A subunit of protein phosphatase 2A, and the signaling kinase TOR1).[11] Proteins containing HEAT-repeats represent about 5% of the human proteome and are widespread in eukaryotes.[12] Despite their low sequence identity, HEAT-repeat proteins share a high structural conservation with the fundamental HEAT-motif being composed of two antiparallel and amphiphilic α-helices linked by intermotif loops, while the HEAT-repeats themselves are connected by one turn.[13,14] Their extended and highly flexible structure enables HEAT-repeat proteins to accommodate and plastically respond to various binding partners. SF3B1 is indeed the assembly platform of several key SPL proteins.[15−17] Owing to their exceptional plasticity, HEAT-repeat proteins

Received: May 22, 2023
Accepted: June 29, 2023
Published: July 3, 2023

https://doi.org/10.1021/acs.jpclett.3c01402
J. Phys. Chem. Lett. 2023, 14, 6263−6269

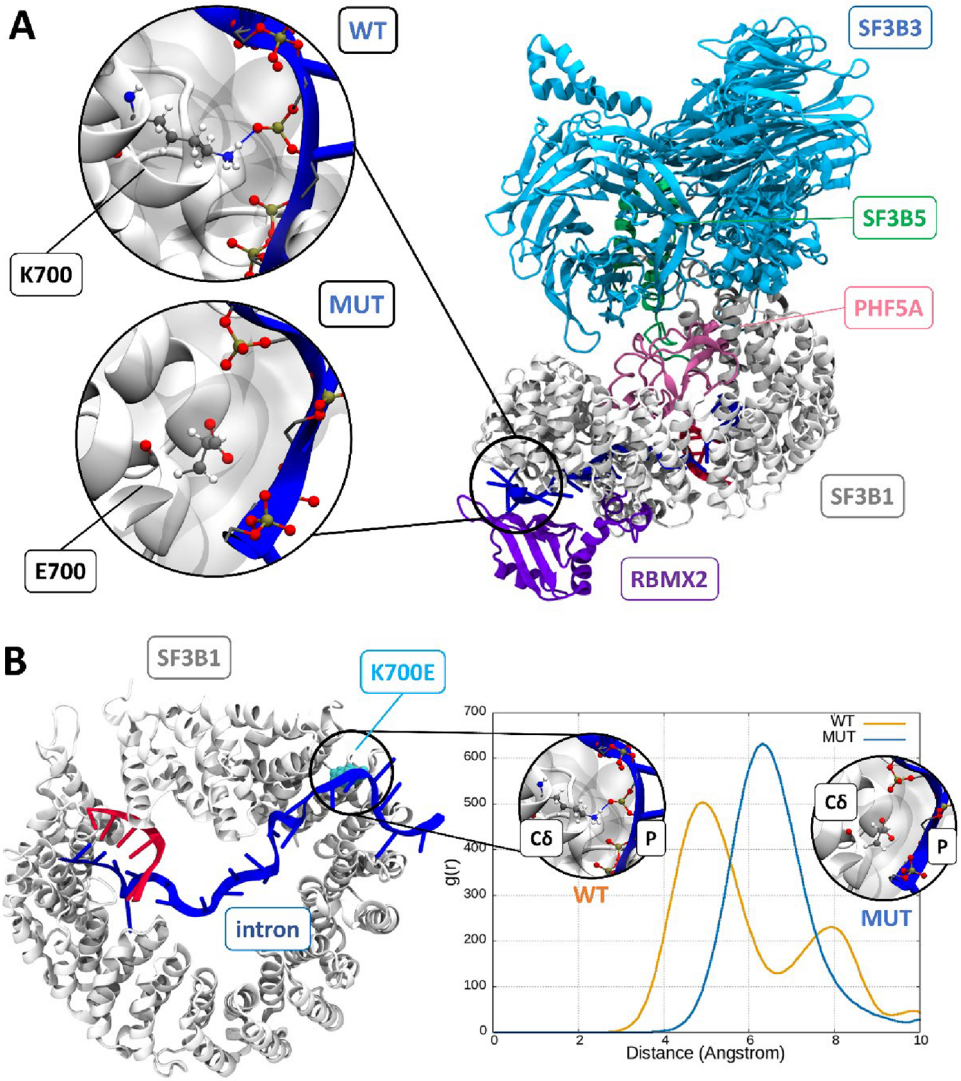

Figure 1. (A) SF3b/pre-mRNA complex (built on PDB code 5Z58)[24] with SF3B1 (white), SF3B3 (cyan), SF3B5 (green), PHF5A (pink), RBMX2 (purple) proteins and pre-mRNA (blue) and U2 (red) are shown as cartoons. Insets (left) show the representative structures extracted from the molecular dynamics (MD) simulations of the system containing wild type (WT) and K700E (MUT) SF3B1. K700, E700, and the RNA phosphate groups are shown in balls-and-sticks. (B) Bottom view of SF3B1. The positions of pre-mRNA and K700E mutation are displayed in cyan van der Waals (vdw) spheres. The radial pair distribution function, $g(r)$, of the distances between K700/E700@Cδ and the intron's phosphate groups is shown for the WT (orange) and MUT (blue) SF3B1. Insets show the presence and absence of hydrogen-bonds between K700@NζH/E700@Oδ and pre-mRNA phosphates.

are also susceptible to mutation-induced structural perturbations. Consistently, SF3B1 is the most frequently mutated splicing factor in the spliceosome.[18] K700E, the most recurrent cancer-associated mutation of SF3B1 (Figure S1),[19] was shown to increase selection of cryptic 3′ splice sites,[18] leading to aberrantly spliced pre-mRNA.[20] Most of the recurrent SF3B1 mutations affect the hydrogen-bonding/salt-bridging ability of the wild-type residue.[21] However, the molecular basis of mutation-induced aberrant 3′ splice site selection remains elusive.[6,18,22,23]

To decrypt the molecular mechanisms underpinning aberrant 3′splice site selection in the presence of the K700E mutation, we established the impact of K700E mutation on pre-mRNA recognition by coupling all-atom molecular dynamics (MD) simulations with dynamical network theory analysis (NWA).[25,26] To this aim, we performed 1 μs long MD simulations on two SF3b models containing the wild type or K700E SF3B1 protein (hereafter named as WT and MUT, Figures 1A and S2). An attentive inspection of the resulting MD simulation trajectories revealed that while in the WT model K700 establishes persistent salt-bridges with several pre-mRNA phosphates, in MUT the negative charge of E700 disrupts these interactions (Figure 1A). This induces a local remodeling of the RNA-SF3B1 hydrogen-bonding pattern, which thrusts the pre-mRNA backbone further away from E700 (Figure S3), as shown by the radial pair distribution function, $g(r)$, of the pre-mRNA's phosphates with respect to K700/E700@Cδ (Figure 1B).

Since the SF3B1 HEAT-repeat motifs were previously suggested to plastically modulate a cross-talk between the K700E mutation and the BPA recognition site,[22] we inspected whether the mutation-induced local remodeling could propagate along the SF3B1 solenoid until the BPA binding site. We observed that E700 alters the flexibility of SF3B1 HEAT-repeat H5−H8 and H16−H17, flanking the mutation site and lining the BPA pocket, respectively (Figure S4). These

https://doi.org/10.1021/acs.jpclett.3c01402
J. Phys. Chem. Lett. 2023, 14, 6263−6269

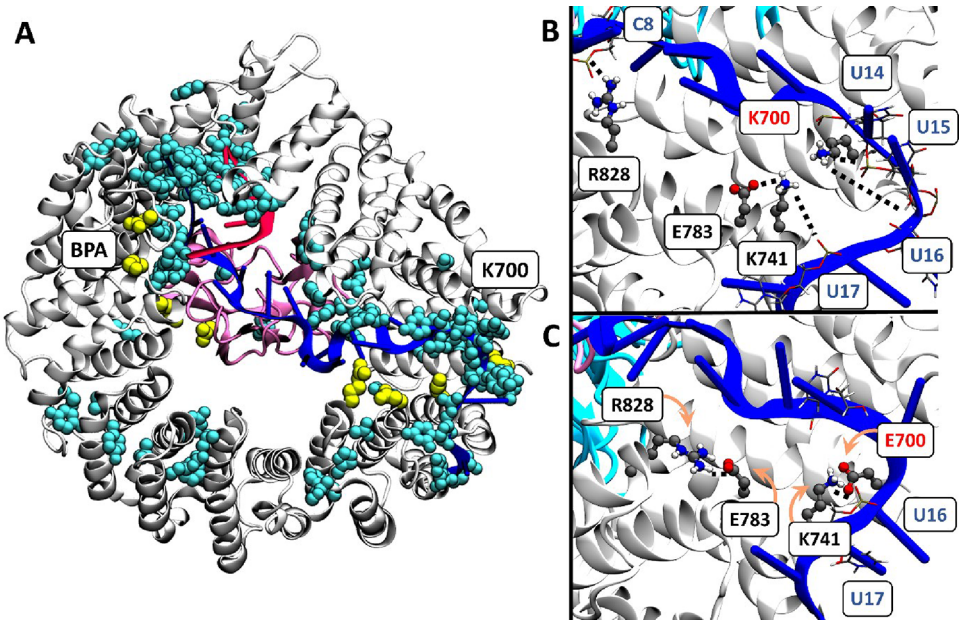

Figure 2. (A) Bottom view of SF3B1/PHF5A showing key interactions differing between WT and MUT models. In cyan (hydrophobic) and yellow (salt bridges), van der Waals spheres highlight the residues whose interactions differ in the two models. The SF3B1 (white), PHF5A (pink), and pre-mRNA (blue) and U2 (red) are shown as cartoons. (B) Close-up of the salt-bridge interactions around K700 in WT and (C) E700 in MUT. The mutated residue E700 interacts with K741, which disrupts the K741-E783 interaction seen in the WT structure. Residues are shown in ball-and-sticks, while pre-mRNA nucleotides are shown in licorice representation. Interactions are marked by black and gray dashed lines.

findings were also supported by an analysis of the cross-correlation matrices, showing more homogeneously correlated motions in these HEAT-repeats and along the SF3B1 solenoid (Figure S5). Next, to obtain a more comprehensive picture of the SF3b/pre-mRNA remodeling, we performed a systematic analysis of all intra- and intermolecular hydrophobic interactions, hydrogen bonds, and salt-bridges in order to identify the residues establishing different interactions in the WT and MUT systems. We observed two big clusters of residues placed nearby K700E and BPA binding pockets (Figure 2A), a finding that further supports the existence of a cross-talk between these sites. Yet, some residues changing their interaction pattern are also located along the pre-mRNA strand due to altered protein/RNA interactions. Of note is the salt-bridge network (Table S1), which, in WT, connects K700 with the U14 phosphate backbone (here BPA is numbered as zero), U15 and U16 bases, and the salt-bridge engaged by R828 with C8 phosphate. Additionally, in WT K741 and E783 form a low-occupancy salt bridge (Figure 2B). Due to the electrostatic repulsion of E700 carboxylic moiety with the pre-mRNA phosphate groups, in MUT, E700 engages a salt bridge with K741 and, in turn, E783 forms a stable salt-bridge with R828. Hence the latter can no longer interact with C8 backbone. This set of switched interactions contributes to propagating the local pre-mRNA destabilization over a large distance (Figure 2C).

One of the residues undergoing the largest variation of the interaction pattern between WT and MUT simulations is R105@RBMX2 (Figure S6). This protein is part of the Retention and Splicing (RES) complex which, by selectively recognizing and binding the polypyrimidine tract, promotes the correct formation of the spliceosome B^{act} complex.[27] Interestingly, nearby RBMX2 and the K700E mutation site, the polypyrimidine tract adopts a marked bend (centered on U15 of pre-mRNA, Figure 3A), which is maintained throughout all MD simulations. This bending could be important for the proper selection of the BPA; unfortunately, to date, no other structural data are available on the pre-mRNA binding with the human SF3b complex. However, a similar bent conformation is also observed in the homologous splicing factor obtained from *Saccharomyces cerevisiae*.

In the WT, R105@RBMX2 engages stable salt-bridges with the phosphate group of U16, strongly anchoring the pre-mRNA strand to SF3B1 (Figure 3B,E). We believe that this salt-bridge, along with those formed by K700 with U14, U15, and U16, contributes to tweeze and maintain pre-mRNA in this bent conformation (Figure 3B). In MUT, the salt-bridges between K700 and the pre-mRNA are lost, triggering an intron shift and remodeling of the R105@RBMX2 salt-bridge network (Figure 3C,D). Owing to the lack of the stable K700 interaction network, in MUT R105@RBMX2 establishes persistent salt-bridges with U14 and U16 (Figure 3C−E) to preserve the intron bending.

Another key protein of SF3b is PHF5A, placed at the center of the SF3B1 solenoid (Figure 1A), which is also critically involved in pre-mRNA binding. PHF5A contains three zinc-finger motifs, which confer rigidity and are most likely instrumental to anchor pre-mRNA as in other DNA/RNA binding proteins.[28] As a result of the mutation-induced remodeling, the pre-mRNA backbone is also shifted further from zinc-finger 1 (ZF1), flanking the BPA binding site, as revealed by the $g(r)$ of the zinc atom with respect to the phosphonate backbone of pre-mRNA (Figure S7). This also affects the salt-bridge R57@PHF5A-C7@pre-mRNA, which holds the pre-mRNA at the center of the SF3B1 solenoid (Figure S8). The shifting of this residue represents another stepping stone into the propagation of K700E-induced pre-mRNA remodeling between the mutation and the BPA site. Indeed, this residue is also the object of the most recurrent PHF5A cancer-associated mutation (R57C).[29] However, to

https://doi.org/10.1021/acs.jpclett.3c01402
J. Phys. Chem. Lett. 2023, 14, 6263−6269

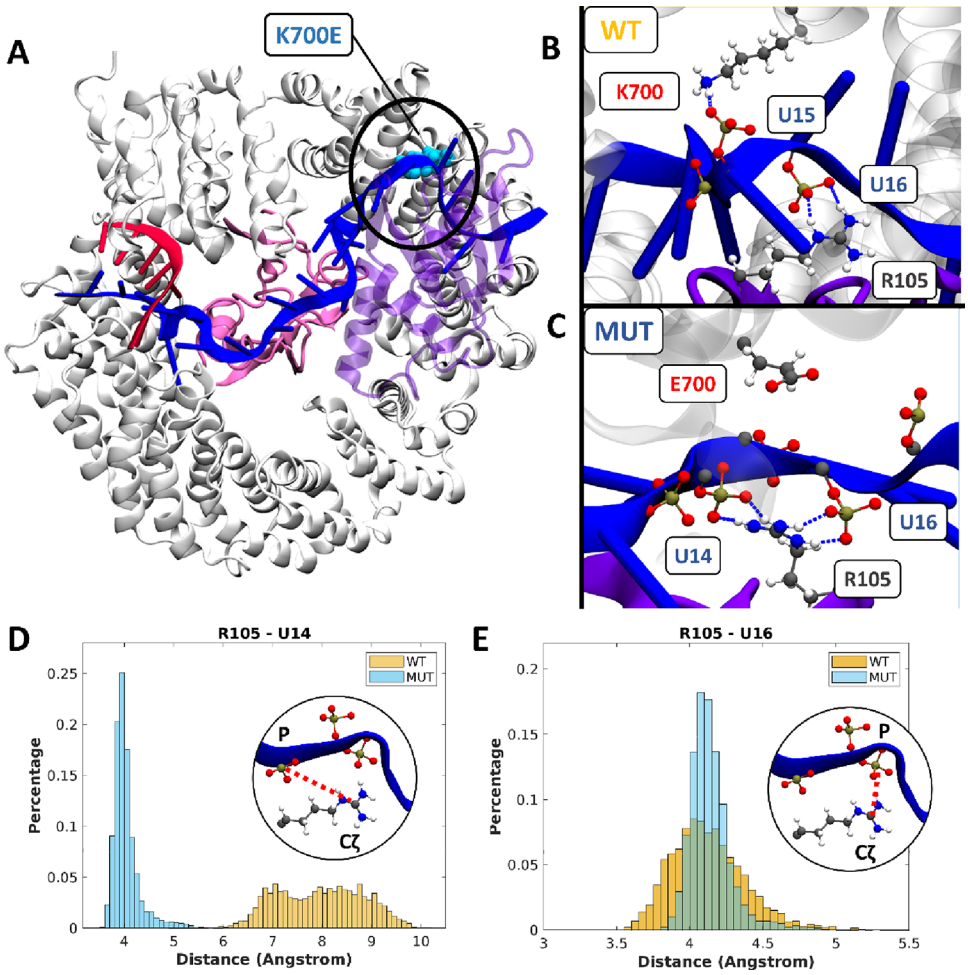

Figure 3. (A) Bottom view of the SF3b complex, highlighting the bending of the pre-mRNA near the K700E mutation site. SF3B1 (white), PHF5A (pink), U2 (red), pre-mRNA (blue), and RBMX2 (purple, transparent) are shown as cartoons. The insets show the salt-bridge network nearby K/E700@SF3B1 and R105@RBMX2 in (B) WT and (C) MUT models, respectively. Residues are shown in ball-and-sticks, while pre-mRNA is shown in blue cartoons. Distance distribution between the guanidium group (Cζ atom) of R105 and the phosphate group (phosphorus atom) of (D) U14 and (E) U16 is shown for the WT (orange line) and the MUT (blue) system. The insets show the distance between the corresponding atoms (Cζ of R105 and P of the phosphate) measured in the corresponding graphs.

the best of our knowledge, no splicing defects are related to this mutation.

Owing to these long-range structural perturbations, we sought to trace the whole signaling-pathways connecting the BPA binding cavity and the K700E mutation site by employing dynamical network theory analysis (NWA) on the WT and MUT models. In NWA, the system is represented as a correlation-based weighted network in which the nodes, indicated by the residues' center of mass, are connected by edges whose weight is proportional to the correlation-strength between residue pairs.[25,26,30] In this manner by computing cross-correlations values between residues along a MD trajectory, NWA traces the optimal (shortest) and suboptimal signaling paths connecting a user-selected source node (here the K700E mutation) to a sink node (R1074 in SF3B1, involved in BPA binding).[31] The resulting path-lengths are thus inversely proportional to the signaling strength and to the amount of correlation existing among their tracing nodes.[6,30] NWA has been proven as a valuable tool to investigate the propagation of allosteric signaling in complex biomolecular systems. Given the importance of these phenomena in controlling many fundamental biological functions, several other state-of-the-art computational techniques are being developed[32] and successfully applied to investigate allosteric modulation in proteins, also in the presence of hotspot mutations.[33,34]

As a result, in WT the signaling-pathways connect K700 and the BPA pocket via PHF5A (Figure 4A), while in MUT, the K700E-induced pre-mRNA remodeling diverts most of them along the SF3B1 solenoid (Figure 4B). This results in longer paths and thus less effective allosteric cross-talk (Figure 4D). Notably, the residues showing the higher degeneracy (which accounts for the number of times a node is present in all paths, Figure 4C) in both systems belong to helix 2 (Figure S9), which, facing the inner part of the SF3B1 ring, allows minimizing the path-length. This finding is consistent with the perturbation of the intra HEAT-repeat interactions detailed above (Figures 2A and S6).

Next, we checked if the high-degeneracy nodes (i.e., those present in more than 75% of all signaling-pathways) were conserved in SF3B1 protein homologous of lower eukaryotic systems (Hsh155 in *Saccharomyces cerevisiae* and the U2 snRNP component prp10 of *Schizosaccharomyces pombe*). Remarkably, nearly all degenerate nodes observed in WT are conserved also in SF3B1 orthologs, while the degree of conservation vanishes in MUT (Table S2).

https://doi.org/10.1021/acs.jpclett.3c01402
J. Phys. Chem. Lett. 2023, 14, 6263−6269

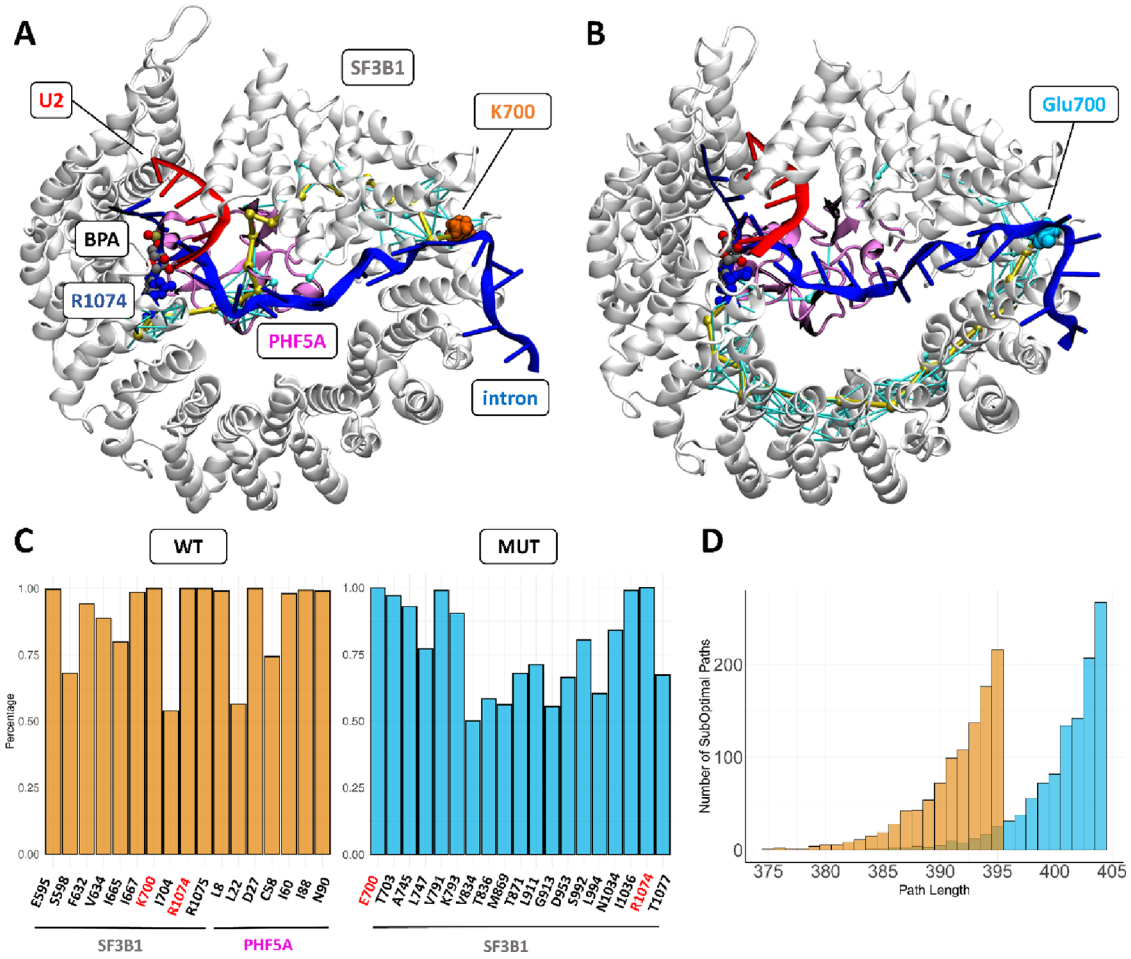

Figure 4. Optimal (thick yellow line) and suboptimal signaling-paths (cyan lines), with nodes depicted as spheres, connecting R1074 (blue), a SF3B1 residue contributing to branch-point adenosine (BPA) binding, shown as van der Waals spheres, and K/E700 (orange/cyan) for (A) WT and (B) MUT models. SF3B1 (white) and the PHF5A protein (pink) along with the pre-mRNA (blue strand), and the U2 RNA (red strand) are shown as cartoons. (C) Histograms showing the node degeneracy in the optimal and suboptimal pathways in WT (orange) and MUT (blue) systems. In red are highlighted source and sink residues. (D) Histograms showing the distribution of signaling path-lengths for the WT (orange) and MUT (blue) systems.

Taken together, our results unlock the molecular basis of RNA-mediated signaling across the SF3b complex. Namely, in the WT, pre-mRNA physically links the two SF3B1 solenoid extremities, tracing, via PHF5A, a shortcut, which also enables an allosteric cross-talk between residue 700 and the BPA binding site. We hypothesize that this signal-exchange may regulate the recognition from the BPA site to the downstream signaling sequences (3′ splice site and polypyrimidine tracts) mediated by different splicing factors that also bind to SF3B1. The K700E cancer-associated mutation perturbs the interaction patterns of the charged residues, placed on the HEAT-repeat mutational hotspots, provoking a domino of switched salt-bridged interactions that propagate the K700E-induced local perturbation over large distances. This weakens pre-mRNA binding, potentially altering the splice site recognition. As a result of the remodeling of pre-mRNA interactions in K700E, the information exchange between the mutation and BPA binding site is scrambled, diverting the signaling paths through the SF3B1 solenoid and weakening the signal strength. Hence, allosteric transmission becomes less effective and more error-prone. We posit this effect to be even more pronounced for weakly binding nonconsensus sequences containing cryptic splice sites, where K700E is known to more dramatically hinder splicing fidelity. In this scenario, it is tempting to suggest that this allosteric signaling-disruption may be broadly shared by other SF3B1 mutations, explaining why SF3B1 cancer-related hotspots mostly involve positively charged residues (e.g., R625, K666 and K700, Figure S1). Moreover, a similar mutation-induced altered allosteric cross-talk between different RRM domains of the U2AF2 splicing factor has been recently reported[6] suggesting that this mechanism may be common to other proteins involved in RNA binding/recognition.

Thus, our study broadens the understanding of the mechanisms underlying mutant-induced aberrant splicing and enlightens the malleability of HEAT-repeat proteins in handling RNA processing in health and diseases. With the SF3b complex being a validated target of splicing modulators,[5,35−38] these findings supply intriguing insights and appealing opportunities for correcting SF3b cancer-associated structural/dynamical alterations with small molecules.[31]

■ ASSOCIATED CONTENT

Supporting Information

The Supporting Information is available free of charge at https://pubs.acs.org/doi/10.1021/acs.jpclett.3c01402.

https://doi.org/10.1021/acs.jpclett.3c01402
J. Phys. Chem. Lett. 2023, 14, 6263−6269

Computational details, Figures S1−S9, and Tables S1 and S2 (PDF)

AUTHOR INFORMATION

Corresponding Author

Alessandra Magistrato − *National Research Council of Italy Institute of Materials (CNR-IOM) c/o SISSA, 34136 Trieste, Italy;* orcid.org/0000-0002-2003-1985; Email: alessandra.magistrato@sissa.it

Authors

Angelo Spinello − *Department of Biological, Chemical and Pharmaceutical Sciences and Technologies, University of Palermo, 90128 Palermo, Italy;* orcid.org/0000-0002-8387-8956

Pavel Janos − *National Research Council of Italy Institute of Materials (CNR-IOM) c/o SISSA, 34136 Trieste, Italy;* orcid.org/0000-0002-9068-2652

Riccardo Rozza − *National Research Council of Italy Institute of Materials (CNR-IOM) c/o SISSA, 34136 Trieste, Italy;* orcid.org/0000-0001-6590-4228

Complete contact information is available at: https://pubs.acs.org/10.1021/acs.jpclett.3c01402

Notes

The authors declare no competing financial interest.

ACKNOWLEDGMENTS

A.S. was supported by a FIRC-AIRC "Mario e Valeria Rindi" fellowship for Italy. A.M. thanks the financial support of the Italian Association for Cancer Research (AIRC) (IG Grant 24514). The authors thank CINECA, the Italian supercomputing center, for computational resources via the "IsB21_SPLSeq" grant and Dr. S. Mays for careful reading of the manuscript.

REFERENCES

(1) Papasaikas, P.; Valcarcel, J. The Spliceosome: The Ultimate RNA Chaperone and Sculptor. *Trends Biochem. Sci.* **2016**, *41* (1), 33−45.

(2) Casalino, L.; Palermo, G.; Rothlisberger, U.; Magistrato, A. Who Activates the Nucleophile in Ribozyme Catalysis? An Answer from the Splicing Mechanism of Group II Introns. *J. Am. Chem. Soc.* **2016**, *138* (33), 10374−10377.

(3) Borisek, J.; Magistrato, A. All-Atom Simulations Decrypt the Molecular Terms of RNA Catalysis in the Exon-Ligation Step of the Spliceosome. *ACS Catal.* **2020**, *10* (9), 5328−5334.

(4) Borisek, J.; Casalino, L.; Saltalamacchia, A.; Mays, S. G.; Malcovati, L.; Magistrato, A. Atomic-Level Mechanism of Pre-mRNA Splicing in Health and Disease. *Acc. Chem. Res.* **2021**, *54* (1), 144−154.

(5) Bonnal, S. C.; Lopez-Oreja, I.; Valcarcel, J. Roles and mechanisms of alternative splicing in cancer - implications for care. *Nat. Rev. Clin. Oncol.* **2020**, *17* (8), 457−474.

(6) Rozza, R.; Saltalamacchia, A.; Orrico, C.; Janos, P.; Magistrato, A. All-Atom Simulations Elucidate the Impact of U2AF2 Cancer-Associated Mutations on Pre-mRNA Recognition. *J. Chem. Inf Model* **2022**, *62* (24), 6691−6703.

(7) Agrawal, A. A.; Yu, L.; Smith, P. G.; Buonamici, S. Targeting splicing abnormalities in cancer. *Curr. Opin Genet Dev* **2018**, *48*, 67−74.

(8) Yoshida, K.; Ogawa, S. Splicing factor mutations and cancer. *Wiley Interdiscip Rev. RNA* **2014**, *5* (4), 445−459.

(9) Papaemmanuil, E.; Gerstung, M.; Malcovati, L.; Tauro, S.; Gundem, G.; Van Loo, P.; Yoon, C. J.; Ellis, P.; Wedge, D. C.; Pellagatti, A.; et al. Clinical and biological implications of driver mutations in myelodysplastic syndromes. *Blood* **2013**, *122* (22), 3616−3627.

(10) Cazzola, M.; Rossi, M.; Malcovati, L. Biologic and clinical significance of somatic mutations of SF3B1 in myeloid and lymphoid neoplasms. *Blood* **2013**, *121* (2), 260−269.

(11) Andrade, M. A.; Bork, P. HEAT repeats in the Huntington's disease protein. *Nat. Genet.* **1995**, *11* (2), 115−116.

(12) Kajander, T.; Cortajarena, A. L.; Main, E. R.; Mochrie, S. G.; Regan, L. A new folding paradigm for repeat proteins. *J. Am. Chem. Soc.* **2005**, *127* (29), 10188−10190.

(13) Kappel, C.; Zachariae, U.; Dolker, N.; Grubmuller, H. An unusual hydrophobic core confers extreme flexibility to HEAT repeat proteins. *Biophys. J.* **2010**, *99* (5), 1596−1603.

(14) Grinthal, A.; Adamovic, I.; Weiner, B.; Karplus, M.; Kleckner, N. PR65, the HEAT-repeat scaffold of phosphatase PP2A, is an elastic connector that links force and catalysis. *Proc. Natl. Acad. Sci. U. S. A.* **2010**, *107* (6), 2467−2472.

(15) Cretu, C.; Schmitzova, J.; Ponce-Salvatierra, A.; Dybkov, O.; De Laurentiis, E. I.; Sharma, K.; Will, C. L.; Urlaub, H.; Luhrmann, R.; Pena, V. Molecular Architecture of SF3b and Structural Consequences of Its Cancer-Related Mutations. *Mol. Cell* **2016**, *64* (2), 307−319.

(16) Tholen, J.; Razew, M.; Weis, F.; Galej, W. P. Structural basis of branch site recognition by the human spliceosome. *Science* **2022**, *375* (6576), 50−57.

(17) Yang, F.; Bian, T.; Zhan, X.; Chen, Z.; Xing, Z.; Larsen, N. A.; Zhang, X.; Shi, Y. Mechanisms of the RNA helicases DDX42 and DDX46 in human U2 snRNP assembly. *Nat. Commun.* **2023**, *14* (1), 897.

(18) Darman, R. B.; Seiler, M.; Agrawal, A. A.; Lim, K. H.; Peng, S.; Aird, D.; Bailey, S. L.; Bhavsar, E. B.; Chan, B.; Colla, S.; et al. Cancer-Associated SF3B1 Hotspot Mutations Induce Cryptic 3′ Splice Site Selection through Use of a Different Branch Point. *Cell Rep.* **2015**, *13* (5), 1033−1045.

(19) Papaemmanuil, E.; Cazzola, M.; Boultwood, J.; Malcovati, L.; Vyas, P.; Bowen, D.; Pellagatti, A.; Wainscoat, J. S.; Hellstrom-Lindberg, E.; Gambacorti-Passerini, C.; et al. Somatic SF3B1 mutation in myelodysplasia with ring sideroblasts. *N. Engl. J. Med.* **2011**, *365* (15), 1384−1395.

(20) Obeng, E. A.; Chappell, R. J.; Seiler, M.; Chen, M. C.; Campagna, D. R.; Schmidt, P. J.; Schneider, R. K.; Lord, A. M.; Wang, L.; Gambe, R. G.; et al. Physiologic Expression of Sf3b1(K700E) Causes Impaired Erythropoiesis, Aberrant Splicing, and Sensitivity to Therapeutic Spliceosome Modulation. *Cancer Cell* **2016**, *30* (3), 404−417.

(21) Kielkopf, C. L. Insights from structures of cancer-relevant pre-mRNA splicing factors. *Curr. Opin. Genet. Dev.* **2018**, *48*, 57−66.

(22) Borisek, J.; Saltalamacchia, A.; Galli, A.; Palermo, G.; Molteni, E.; Malcovati, L.; Magistrato, A. Disclosing the Impact of Carcinogenic SF3b Mutations on Pre-mRNA Recognition Via All-Atom Simulations. *Biomolecules* **2019**, *9* (10), 633.

(23) Samy, A.; Suzek, B. E.; Ozdemir, M. K.; Sensoy, O. In Silico Analysis of a Highly Mutated Gene in Cancer Provides Insight into Abnormal mRNA Splicing: Splicing Factor 3B Subunit 1(K700E) Mutant. *Biomolecules* **2020**, *10* (5), 680.

(24) Zhang, X.; Yan, C.; Zhan, X.; Li, L.; Lei, J.; Shi, Y. Structure of the human activated spliceosome in three conformational states. *Cell Res.* **2018**, *28* (3), 307−322.

(25) Laporte, S.; Magistrato, A. Deciphering the Molecular Terms of Arp2/3 Allosteric Regulation from All-Atom Simulations and Dynamical Network Theory. *J. Phys. Chem. Lett.* **2021**, *12* (22), 5384−5389.

(26) Saltalamacchia, A.; Casalino, L.; Borisek, J.; Batista, V. S.; Rivalta, I.; Magistrato, A. Decrypting the Information Exchange Pathways across the Spliceosome Machinery. *J. Am. Chem. Soc.* **2020**, *142* (18), 8403−8411.

(27) Bao, P.; Will, C. L.; Urlaub, H.; Boon, K. L.; Luhrmann, R. The RES complex is required for efficient transformation of the

precatalytic B spliceosome into an activated B(act) complex. *Genes Dev.* **2017**, *31* (23−24), 2416−2429.
(28) Cassandri, M.; Smirnov, A.; Novelli, F.; Pitolli, C.; Agostini, M.; Malewicz, M.; Melino, G.; Raschella, G. Zinc-finger proteins in health and disease. *Cell Death Discovery* **2017**, *3*, 17071.
(29) Puente, X. S.; Pinyol, M.; Quesada, V.; Conde, L.; Ordonez, G. R.; Villamor, N.; Escaramis, G.; Jares, P.; Bea, S.; Gonzalez-Diaz, M.; et al. Whole-genome sequencing identifies recurrent mutations in chronic lymphocytic leukaemia. *Nature* **2011**, *475* (7354), 101−105.
(30) Melo, M. C. R.; Bernardi, R. C.; de la Fuente-Nunez, C.; Luthey-Schulten, Z. Generalized correlation-based dynamical network analysis: a new high-performance approach for identifying allosteric communications in molecular dynamics trajectories. *J. Chem. Phys.* **2020**, *153* (13), 134104.
(31) Borisek, J.; Saltalamacchia, A.; Spinello, A.; Magistrato, A. Exploiting Cryo-EM Structural Information and All-Atom Simulations To Decrypt the Molecular Mechanism of Splicing Modulators. *J. Chem. Inf. Model.* **2020**, *60*, 2510.
(32) Arantes, P. R.; Patel, A. C.; Palermo, G. Emerging Methods and Applications to Decrypt Allostery in Proteins and Nucleic Acids. *J. Mol. Biol.* **2022**, *434* (17), 167518.
(33) Morra, G.; Colombo, G. Relationship between energy distribution and fold stability: Insights from molecular dynamics simulations of native and mutant proteins. *Proteins* **2008**, *72* (2), 660−672.
(34) Moroni, E.; Agard, D. A.; Colombo, G. The Structural Asymmetry of Mitochondrial Hsp90 (Trap1) Determines Fine Tuning of Functional Dynamics. *J. Chem. Theory Comput.* **2018**, *14* (2), 1033−1044.
(35) Seiler, M.; Yoshimi, A.; Darman, R.; Chan, B.; Keaney, G.; Thomas, M.; Agrawal, A. A.; Caleb, B.; Csibi, A.; Sean, E.; et al. H3B-8800, an orally available small-molecule splicing modulator, induces lethality in spliceosome-mutant cancers. *Nat. Med.* **2018**, *24* (4), 497−504.
(36) Spinello, A.; Borisek, J.; Malcovati, L.; Magistrato, A. Investigating the Molecular Mechanism of H3B-8800: A Splicing Modulator Inducing Preferential Lethality in Spliceosome-Mutant Cancers. *Int. J. Mol. Sci.* **2021**, *22* (20), 11222.
(37) Rozza, R.; Janos, P.; Spinello, A.; Magistrato, A. Role of computational and structural biology in the development of small-molecule modulators of the spliceosome. *Expert Opin. Drug Discovery* **2022**, *17* (10), 1095−1109.
(38) Borisek, J.; Aupic, J.; Magistrato, A. Establishing the catalytic and regulatory mechanism of RNA-based machineries. *Wires Comput. Mol. Sci.* **2023**, *13* (3), e1643.

https://doi.org/10.1021/acs.jpclett.3c01402
J. Phys. Chem. Lett. 2023, 14, 6263−6269